

High-pressure synchrotron radiation diffraction studies of icosahedral Ti-Zr-Ni and hydrogenated Ti-Zr-Ni quasicrystals

This article has been downloaded from IOPscience. Please scroll down to see the full text article.

2001 J. Phys.: Condens. Matter 13 8527

(<http://iopscience.iop.org/0953-8984/13/37/310>)

View [the table of contents for this issue](#), or go to the [journal homepage](#) for more

Download details:

IP Address: 171.66.16.226

The article was downloaded on 16/05/2010 at 14:52

Please note that [terms and conditions apply](#).

High-pressure synchrotron radiation diffraction studies of icosahedral Ti–Zr–Ni and hydrogenated Ti–Zr–Ni quasicrystals

A Sadoc^{1,2,5}, J P Itié^{2,3}, A Polian^{2,3}, J Y Kim⁴ and K F Kelton⁴

¹ Laboratoire de Physique des Matériaux et des Surfaces, Université de Cergy-Pontoise, 5 Mail Gay Lussac, Neuville sur Oise, 95031 Cergy-Pontoise Cédex, France

² LURE, CNRS, MESR, CEA, Centre Universitaire Paris-Sud, BP 34, 91898 Orsay Cédex, France

³ Physique des Milieux Condensés, Université Pierre et Marie Curie, CNRS UMR 76 02, 75252 Paris Cédex 05, France

⁴ Department of Physics, Washington University, St Louis, MO 63130, USA

E-mail: anne.sadoc@lpms.u-cergy.fr

Received 3 April 2001, in final form 8 June 2001

Published 30 August 2001

Online at stacks.iop.org/JPhysCM/13/8527

Abstract

We present results from *in situ* x-ray diffraction studies of hydrogenated icosahedral Ti–Zr–Ni quasicrystals carried out under high pressure. The icosahedral $\text{Ti}_{53}\text{Zr}_{27}\text{Ni}_{20}$ phase and hydrogenated icosahedral $\text{Ti}_{45}\text{Zr}_{38}\text{Ni}_{17}$ samples that contain 0.32 and 1.45 hydrogen atoms for each metal atom were studied. The icosahedral quasicrystal structure is retained up to the highest pressures investigated. The six-dimensional lattice parameter was obtained as a function of pressure for the different samples. The zero-pressure bulk modulus and its pressure derivative were determined by fitting a Murnaghan-type equation of state to the relative volume change V/V_0 . The zero-pressure bulk modulus is respectively obtained as $B_0 = 130 \pm 10$, 105 ± 10 , and 110 ± 20 GPa for H/M equal to 0, 0.32, and 1.45 using a constant value for the first derivative B'_0 : 5.5 ± 1 . It seems, therefore, that the icosahedral Ti–Zr–Ni phase may be more compressible after hydrogenation, but there is no clear difference for different H/M contents. These results are tentatively related to the local structure of these materials.

1. Introduction

Because of their ability to reversibly absorb significant quantities of hydrogen, crystalline and amorphous transition metals and their alloys have been extensively studied with a view to potential use in hydrogen storage applications. Key factors for determining which materials

⁵ Author to whom any correspondence should be addressed. Telephone: +33 (0)1 34257028; fax: +33 (0)1 34257071.

can store hydrogen include the chemical interactions between metal and hydrogen atoms and the number, type, and size of interstitial sites in the host metal. In most transition metal alloys, the hydrogen prefers to sit at tetrahedrally coordinated sites, making the icosahedral quasicrystals (QCs), dominated by local tetrahedral order, particularly attractive. Ti- and Zr-based QCs have already been observed to store hydrogen up to a content close to those of the best crystalline materials [1, 2]. The most exciting feature of the new Ti/Zr-based quasicrystals is their ability to reversibly store hydrogen [3], thus opening up a promising new field for application.

While many studies have been devoted to the temperature stability of hydrogenated Ti/Zr-based QCs, there have been none concerning the high-pressure behaviour of these materials. Nevertheless, the stability under pressure is important for sintering processes and various high-pressure synthesis procedures. Therefore, we have undertaken a study by means of x-ray diffraction of the high-pressure properties of hydrogenated Ti–Zr–Ni phases in quasihydrostatic conditions and compared the results to those obtained for the icosahedral non-hydrogenated Ti–Zr–Ni phase. In fact, very recent high-pressure studies on Ti–Zr–Ni have shown that this material is stable up to pressures of 30 GPa [4–6].

In this paper, *in situ* x-ray diffraction studies on hydrogenated icosahedral Ti–Zr–Ni quasicrystals under high pressure and under quasihydrostatic conditions are reported for the first time. The icosahedral $\text{Ti}_{53}\text{Zr}_{27}\text{Ni}_{20}$ phase (Ti–Zr–Ni) and icosahedral $\text{Ti}_{45}\text{Zr}_{38}\text{Ni}_{17}$ phases that also contain 0.32 and 1.45 hydrogen atoms for each metal atom (Ti–Zr–Ni + H) were investigated. Preliminary results have been briefly reported elsewhere [6, 7]. This paper is organized as follows. In section 2, alloy preparation and the synchrotron radiation diffraction experiments are described. Section 3 is devoted to the data analysis, while results are presented in section 4 and discussed in section 5. The conclusions are summarized in section 6.

2. Experimental procedure

Samples of the icosahedral phase $\text{Ti}_{53}\text{Zr}_{27}\text{Ni}_{20}$ (Ti–Zr–Ni) and samples of icosahedral $\text{Ti}_{45}\text{Zr}_{38}\text{Ni}_{17}$ (Ti–Zr–Ni + 0.32H and Ti–Zr–Ni + 1.45H) that contain approximately 0.32 and 1.45 hydrogen atoms for each metal atom ($H/M = 0.32$ and 1.45) were prepared and characterized at Washington University (St Louis, MO). Rapidly quenched ribbons of the quasicrystals were produced by melt-spinning onto a copper wheel. The resulting $\text{Ti}_{45}\text{Zr}_{38}\text{Ni}_{17}$ i-phase ribbons were plasma-etched, coated with a thin layer of Pd, and hydrogenated by direct exposure to hydrogen gas [8, 9] to an H/M value of approximately 0.32 and 1.45. Small flakes of $\text{Ti}_{53}\text{Zr}_{27}\text{Ni}_{20}$ ribbons and some grains of Ti–Zr–Ni + H fine-grained powder were used for the high-pressure diffraction experiments.

The x-ray diffraction experiments were carried out at the Laboratoire pour l'Utilisation du Rayonnement Electromagnétique (LURE, Orsay) using the DCI synchrotron radiation facility. They were recorded on the experimental station DW11, which uses the white beam of the 5 T wiggler. The incident beam was collimated down to $50 \times 50 \mu\text{m}$ using crossed slits. The experiments were performed in the energy-dispersive mode, using a germanium solid-state detector, the resolution of which is 250 eV at 20 keV. The Bragg relation between the interplanar distance d and the energy E is given by

$$d \text{ (\AA)} = \frac{12.398}{2(\sin \theta)E \text{ (keV)}} \quad (1)$$

where θ is the angle between the incident x-ray beam and the sample plane. This angle, close to 6° , is chosen in order to obtain the most interesting peaks of the icosahedral structure in the 15–30 keV energy range, where the intensity of the incident beam is a maximum. θ is fixed and

its value is obtained from measurements of the interplanar spacings at atmospheric pressure (or 'zero' pressure) of a reference compound, a copper foil. The product Ed is therefore a constant, C :

$$C = \frac{12.398}{2 \sin \theta}.$$

The beam passed through the high-pressure cell, a membrane diamond-anvil cell [10] with a stainless steel gasket. In order to obtain quasihydrostatic conditions, nitrogen was used as a pressure-transmitting medium inside the diamond-anvil cell for Ti–Zr–Ni and Ti–Zr–Ni + 0.32 H samples and helium for Ti–Zr–Ni + 1.45 H. In fact, one diamond was found to be cracked after use of nitrogen, which had diffused into the diamonds and weakened them. Therefore, helium was used instead of nitrogen for the following experiment, i.e. for the H/M = 1.45 sample. Unfortunately, one diamond broke at 7 GPa. The pressure, P , was determined by the wavelength shift of the R1 fluorescence line of a ruby chip situated near to the sample, using a linear scale [11]. The diffraction pattern was recorded at ambient pressure and from 1.3 GPa to 26 GPa for Ti–Zr–Ni, from 3 GPa to 15 GPa in the case of Ti–Zr–Ni + 0.32 H, from 0.7 GPa to 7.2 GPa in the case of Ti–Zr–Ni + 1.45 H, and also at ambient pressure after coming back to zero pressure ($0d$) after the high-pressure cycle. For the Ti–Zr–Ni flake, the sample was observed from time to time in a microscope, in order to check the state of the gasket. It was noted that the flake kept the same shape up to the highest pressure.

Owing to the size of the beam ($50 \times 50 \mu\text{m}$) and to the small amount of sample in the diamond-anvil cell, the number of grains which can diffract is very small. This technique is therefore sensitive to the orientation of the sample. The mean positions of the Bragg peaks are not affected, but the intensities are not very reliable due to the lack of true powder distribution. Moreover, some not very intense reflections may or may not appear in the diffraction pattern of the QCs.

3. Data analysis

Quasicrystalline structures are quasiperiodic and therefore can be described as irrational cuts of strictly periodic objects in a high-dimension space $E = E_{\parallel} \oplus E_{\perp}$, where E_{\parallel} is the physical space and E_{\perp} the perpendicular space. For icosahedral quasicrystals, the hyperspace has minimal dimension 6. The indexing of the diffraction patterns has been performed in the six-dimensional (6D) scheme proposed by Cahn, Shechtman, and Gratias [12]. In that scheme, two integers N and M are used for labelling the reflections in the powder diffraction patterns. A reflection labelled (N, M) is located in reciprocal space at

$$|Q_{\parallel}| = \frac{1}{A} \frac{\sqrt{N + M\tau}}{\sqrt{2(2 + \tau)}} \quad (2)$$

and

$$|Q_{\perp}| = \frac{1}{A} \frac{\sqrt{\tau(N\tau - M)}}{\sqrt{2(2 + \tau)}} \quad (3)$$

where τ is the golden mean, $\tau = (1 + \sqrt{5})/2$, A is the six-dimensional lattice parameter, and Q_{\parallel} and Q_{\perp} are the projections in parallel and perpendicular spaces of a 6D reciprocal-lattice vector, Q . According to equation (2), A is given by

$$A = \frac{1}{|Q_{\parallel}|} \frac{(N + M)^{1/2}}{[2(2 + \tau)]^{1/2}}. \quad (4)$$

$|Q_{\parallel}|$ is equal to the inverse of the interplanar distance d . According to equations (1) and (4), the lattice parameter A can be derived, for each (N, M) Bragg peak, from the peak positions in the energy scale using

$$A = \frac{C (N + M\tau)^{1/2}}{E [2(2 + \tau)]^{1/2}} \quad (5)$$

where C is the constant determined for the copper foil. Four Bragg peaks were measured: (18, 29), (20, 32), (26, 41), and (52, 84). For each diffraction pattern, the position, the intensity, and the width at half-maximum (FWHM) of each Bragg peak were determined using the program *edx* [13].

As the first effect of pressure is to reduce the lattice parameter, it is possible, from the diffraction data, to obtain the compressibility of the material. In fact, it is more convenient to use the inverse of the compressibility—that is, the bulk modulus B —to determine the equation of state:

$$B = -V \left(\frac{dP}{dV} \right). \quad (6)$$

In a first approximation, B is taken as a linear function of P :

$$B = B_0 + B'_0 P \quad (7)$$

where B_0 , the bulk modulus at zero pressure, and B'_0 , its first derivative, are related to the elastic constants of the sample. They can also be used to help to assess, and even reject, theoretical models. By integration of equation (6), one obtains the Murnaghan equation of state [14]:

$$\frac{V}{V_0} = \left(1 + \frac{B'_0 P}{B_0} \right)^{-1/B'_0}. \quad (8)$$

In the present case, V/V_0 was taken equal to $(A/A_0)^3$, V_0 and A_0 being respectively the values at ambient pressure of the volume V and of the hypercubic lattice parameter A .

4. Results

Diffraction patterns are shown versus the energy in figure 1 and in figure 2 for Ti–Zr–Ni and Ti–Zr–Ni + 0.32H with the indexing. Similar spectra were obtained for the small set of data for the 1.45 H alloy. Besides the main (18, 29), (20, 32), (26, 41), and (52, 84) diffraction lines, less intense peaks were observed from time to time due to preferential crystallographic orientation of the powder or of the gasket. Moreover, at about 8 GPa, two peaks appeared, in the 20–23 keV energy range, for Ti–Zr–Ni + 0.32H (figure 2). They have decreased or even disappeared by the highest pressure P , 15 GPa. As they shift more rapidly toward high energies than the main Bragg peaks, they could not be due to the powder sample, but are probably due to the pressure-transmitting medium, i.e. solid nitrogen. The (18, 29), (20, 32), (26, 41), and (52, 84) Bragg peaks shift monotonically to higher E -values when the pressure increases. After release of pressure, the Bragg peaks recover their initial position as shown in figure 3 for Ti–Zr–Ni. The spectrum obtained before the high-pressure cycle appears more noisy than that taken after coming back to ambient pressure, because it was taken over only 15 minutes while the latter was recorded over several hours. It is worth remarking that the main (18, 29) and (20, 32) diffraction lines are well separated, not only at ambient pressure, but also throughout the whole pressure cycle and also after coming back to zero pressure. The widths of the Bragg peaks are larger than 400 eV at ambient pressure and increase with increasing pressure, but by no more than about 100 eV up to the highest pressure. After

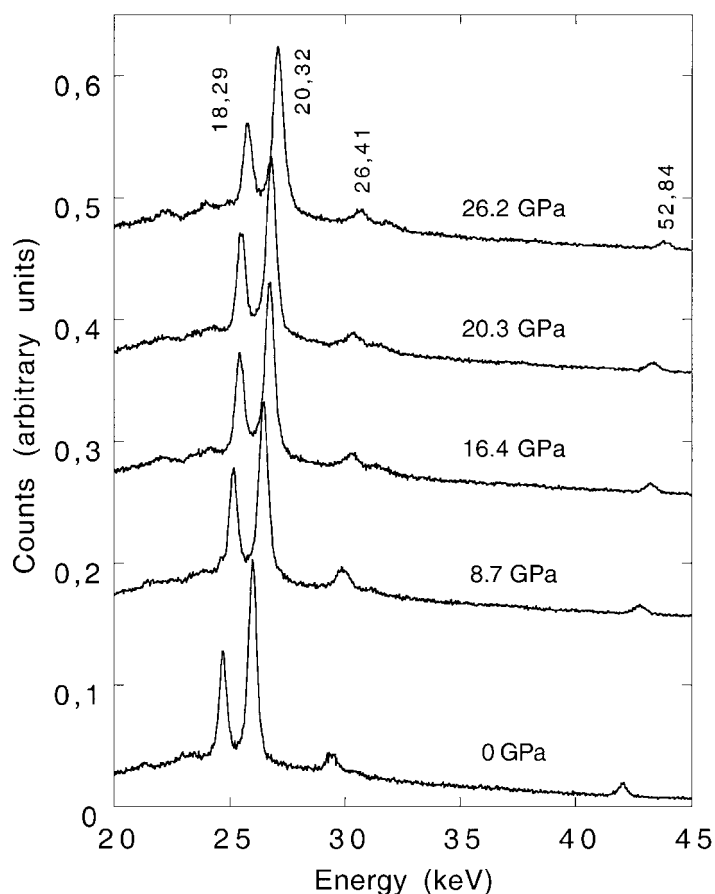


Figure 1. X-ray diffraction spectra of Ti–Zr–Ni versus energy, from ambient pressure (bottom) up to 26 GPa; the Bragg peaks are indexed following Cahn *et al* [12].

coming back to zero pressure, they remained somewhat broadened due to some pressure-induced defects, which are frozen upon pressure release. As the icosahedral Ti–Zr–Ni phases are not perfect quasicrystals, like icosahedral AlCuFe, AlCuRu, or AlPdMn, we have not studied in detail the broadening of the Bragg peaks which appears systematically in QCs under pressure [15, 16].

The diffraction patterns were then analysed using peak-fitting and profile-deconvolution procedures. Indexing of the diffraction lines of the zero-pressure samples led to the following values of the hypercubic lattice parameter: $A_0 = 7.232 \text{ \AA}$, 7.434 \AA , and 7.7080 \AA for H/M respectively equal to 0, 0.32, and 1.45.

A question of particular interest is that of whether the samples exhibit anisotropic elasticity. To answer this question, we have plotted the pressure dependence of the ratio A/A_0 for each type of Bragg peak. A similar evolution is obtained for the different peaks as exemplified in figure 4. Therefore, the compressibility is equivalent in all directions and there was no uniaxial component. This checks that the experiments were performed under homogeneous stress conditions. Moreover, the compression of the 6D cubic lattice is found to be isotropic, like in previously studied QCs, and the icosahedral phase remains cubic in six dimensions under high pressure.

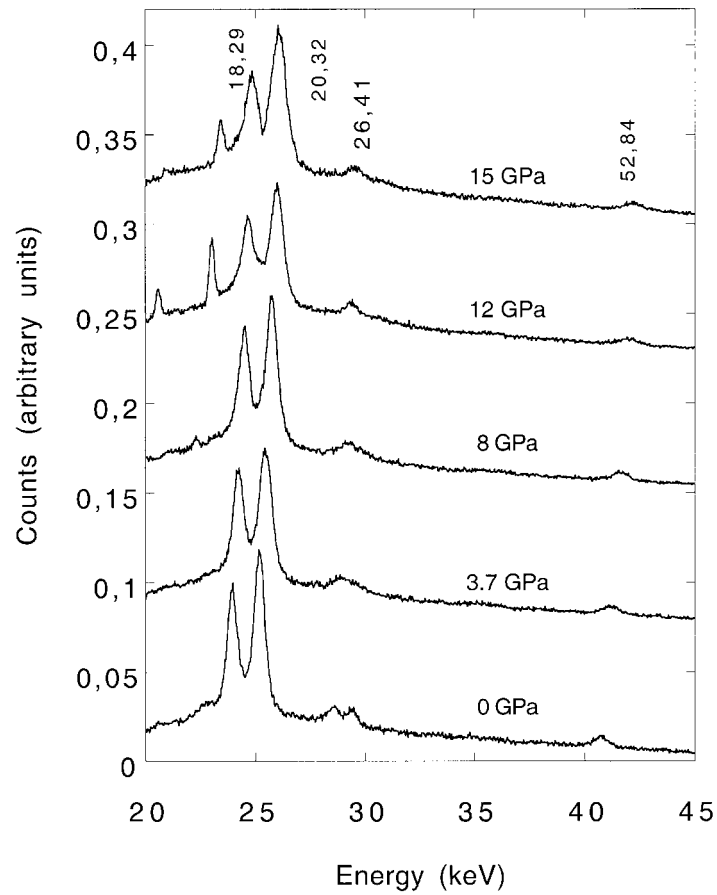


Figure 2. X-ray diffraction spectra of Ti-Zr-Ni + 0.32 H versus energy, from ambient pressure (bottom) up to 15 GPa.

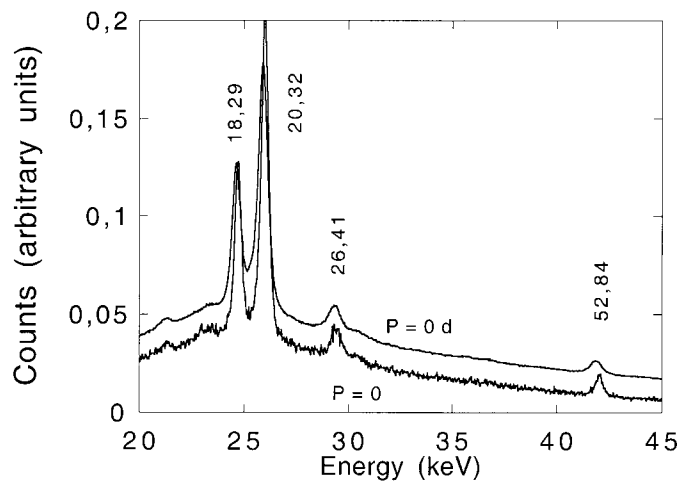


Figure 3. A plot of the energy-dispersive spectra at atmospheric pressure before compression (bottom) and after the high-pressure cycle (top) for Ti-Zr-Ni.

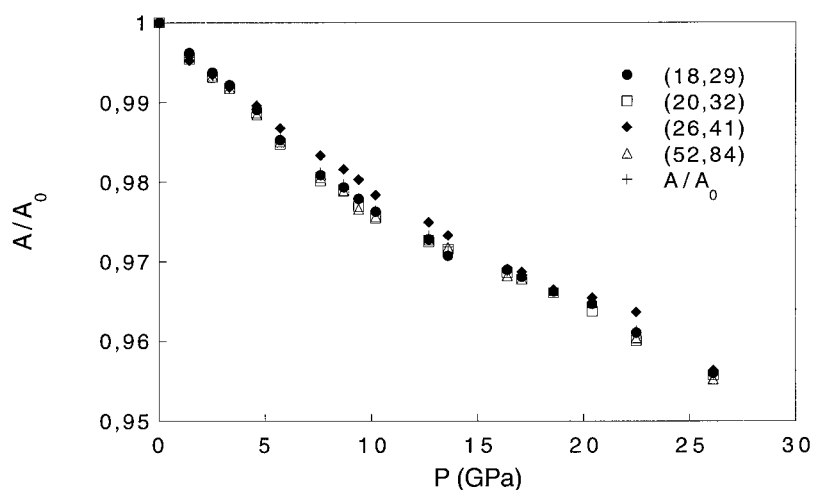


Figure 4. Relative variation of the 6D parameter for the (18, 29), (20, 32), (26, 41), and (52, 84) reflections and for their average for Ti–Zr–Ni.

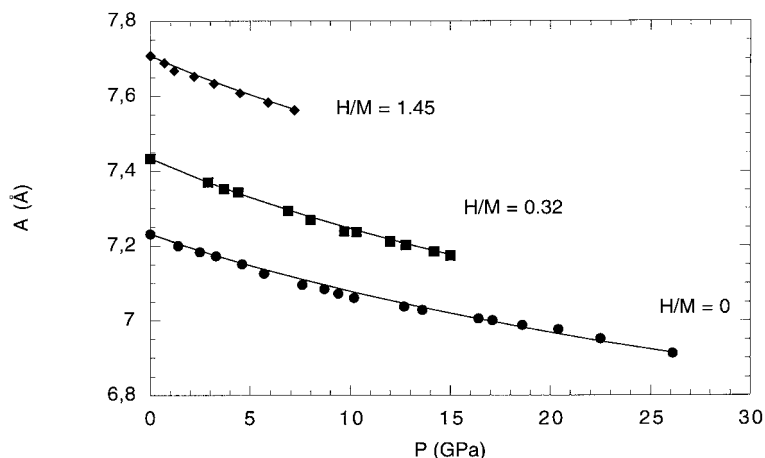


Figure 5. Variation of the six-dimensional parameter versus pressure in Ti–Zr–Ni for different values of H/M (0, 0.32, and 1.45). Solid lines: Murnaghan fits.

The pressure dependence of the 6D parameters is given in figure 5. They decrease monotonically with increasing P showing the stability of the icosahedral phases. From the average lattice parameter, one obtains the relative variation V/V_0 (figure 6). The inset of figure 6 shows an enlarged view of the low-pressure range. The curves for A or V/V_0 are well fitted by a Murnaghan equation of state up to the highest pressure, for a constant value of the B'_0 -derivative, equal to 5.5 ± 1 , using $B_0 = 130 \pm 10$ GPa for Ti–Zr–Ni, 105 ± 10 GPa for $H/M = 0.32$, and 110 ± 20 GPa for $H/M = 1.45$. Therefore, the $H/M = 0.32$ sample appears more compressible at ambient pressure than the alloy without hydrogen, as is clearly evident in figure 5. For the $H/M = 1.45$ sample, unfortunately, the number of experimental points is rather limited and differences are difficult to establish. However, in the pressure range where it could be studied, this sample does not appear more compressible than the $H/M = 0.32$ sample (inset of figure 6).

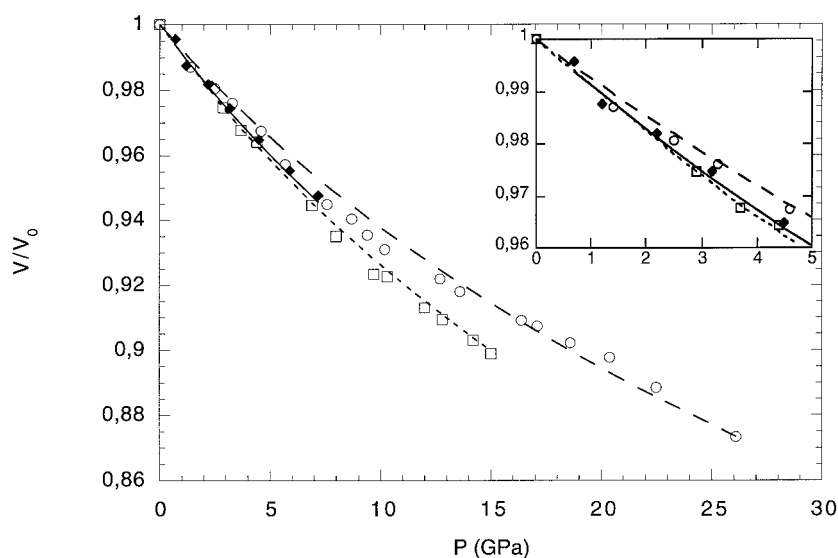


Figure 6. Relative variation of the average volume versus pressure in Ti–Zr–Ni for different values of H/M (0, 0.32, and 1.45). Murnaghan fits: long-dashed line for H/M = 0, dotted line for H/M = 0.32, full line for H/M = 1.45. The inset shows an enlarged view of the low-pressure range.

The value found for the bulk modulus of Ti–Zr–Ni is very similar to those found for icosahedral Al–Pd–Mn ($B_0 = 133$ GPa [17]) and Al–Cu–Ru ($B_0 = 128$ GPa [15, 16]), which are perfect QCs and also stable under high pressure. The behaviour of icosahedral Al–Li–Cu appears very peculiar, with a high compressibility ($B_0 = 71$ GPa) and a pressure-induced phase transition [18–21].

The difference in B_0 -value obtained (105 to 130 GPa) on comparing H/M = 0.32 to H/M = 0 is rather small. The corresponding change for the 6D parameter is about 0.20 Å. For the hydrogenated alloy, a compression of about 11 GPa is necessary to obtain a 0.20 Å change in the 6D parameter. Using the linear equation (7) and $B'_0 = 5.5$ to determine the bulk modulus change corresponding to 11 GPa, one obtains approximately 60 GPa, which is about double the experimentally obtained difference.

5. Discussion

The zero-pressure bulk modulus, B_0 , and its pressure derivative, B'_0 , were evaluated using the pressure–volume data for the whole pressure range and a Murnaghan-type equation of state. The resulting values, $B_0 = 130 \pm 10$ GPa and $B'_0 = 5.5$, obtained for the non-hydrogenated alloy compare well with those obtained for i-AlPdMn [17] using either x-ray diffraction ($B_0 = 133 \pm 5$ GPa, $B'_0 = 5$) or ultrasonic measurements on large good-quality single grains ($B_0 = 128$ GPa with an accuracy of 0.5%, $B'_0 = 4.7$), the sample thickness being 5 to 10 mm for these latter measurements. They differ, however, from the B_0 - and B'_0 -values measured recently by Nicula *et al* [5] using x-ray diffraction in i-Ti_{52.8}Zr_{26.2}Ni₂₁ ($B_0 = 173 \pm 5$ GPa, $B'_0 = 2.3$). This could result from different experimental conditions. In particular, different results could come from the mixing of the two most intense (18, 29) and (20, 32) lines from 8 GPa up to the highest pressure and also after pressure release in the data of Nicula *et al*, while in the present studies these peaks were well separated up to the highest pressure, and also after

pressure release (figures 1 and 3). On the other hand, the present bulk modulus value is closer to the value estimated by Foster *et al* [21] from ultrasonic measurements on $i\text{-Ti}_{41.5}\text{Zr}_{41.5}\text{Ni}_{17}$ parallelepipeds of about 1 to 2 mm on an edge ($B_0 = 111.5$ GPa with an accuracy of 2%). In their study, Foster *et al* made a comparison with literature values for the constituent metals Ti, Zr, and Ni, and a weighted average for $\text{Ti}_{41.5}\text{Zr}_{41.5}\text{Ni}_{17}$ was calculated. It was concluded that the resulting value (115.7 GPa) was almost the same as those measured (111.5 GPa). Using the same method, we have calculated the weighted value for $i\text{-Al}_{68.7}\text{Pd}_{21.7}\text{Mn}_{9.6}$; the resulting value (99.7 GPa) differs, as usual, from those obtained experimentally whatever experimental method was employed ($B_0 = 128$ or 133 GPa) [17]. Therefore, it is remarkable that the weighted average gives almost the experimental value for the Ti–Zr–Ni alloy.

The $H/M = 0.32$ sample appears more compressible at ambient pressure than the hydrogen-free alloy. This agrees with the increase of the lattice parameter at ambient pressure upon hydrogenation. However, there is no clear difference between the B_0 -values for higher H/M content. This could be related to a recent study of hydrogenation of Zr–Cu–Ni–Al QCs [22], where, instead of the continuous increase of the specific volume per hydrogen atom, a decrease was observed at first as a function of the hydrogen content, up to H/M equal to 0.4. This was interpreted as indicating that the first hydrogen atoms expanded not only their interstitial sites, but also the neighbouring, still empty ones. Therefore, during the following charging, occupation of these already expanded sites became easier. This would explain the very small values for the specific volume at higher hydrogen content. This could also simply explain why, in the present study, the compressibility is greater for $H/M = 0.32$ than for $H/M = 1.45$.

Two recent experiments, performed on the same Ti–Zr–Ni QCs, could help towards a better understanding of the results. First, extended x-ray absorption fine-structure (EXAFS) studies of hydrogenated QCs and 1/1 approximant Ti–Zr–Ni alloys have shown that the local structure is disordered after hydrogenation, with the maximum disorder for the highest H/M content [23, 24]. Secondly, nuclear magnetic resonance (NMR) measurements have been performed on icosahedral $\text{Ti}_{45}\text{Zr}_{38}\text{Ni}_{17}$ QCs, and structural models based on the canonical cell-tiling approach have been used to calculate the second moment [25]. The only free parameter in these calculations was the minimum allowed separation for H–H neighbours, d_{min} . Fitting the experimental data required $d_{min} = 1.9$ Å, a value below the accepted Switendick criterion $d_{min} = 2.1$ Å. Therefore, the EXAFS results and the necessity in the NMR calculations of using a small value of d_{min} could indicate that the hydrogenated structure is distorted. These distortions could, in turn, harden the structure and prevent a larger compressibility in the samples with higher H/M content. Anyway, the structure of the hydrogenated alloys is by no means a simple dilation of that of the non-hydrogenated one, since, in this case, the change in the compressibility would be far more important than that observed experimentally, even for the $H/M = 0.32$ sample. This is consistent with the EXAFS results which show that the first interatomic distances do not all change in the same way in the hydrogenated alloy, which should create some distortion in the local order [23, 24].

6. Conclusions

The high-pressure properties of icosahedral $\text{Ti}_{53}\text{Zr}_{27}\text{Ni}_{20}$ samples and icosahedral $\text{Ti}_{45}\text{Zr}_{38}\text{Ni}_{17}$ samples that contain approximately 0.32 and 1.45 hydrogen atoms for each metal atom were investigated using synchrotron radiation energy-dispersive diffraction. These measurements represent the first experimental investigation of the x-ray diffraction of hydrogenated icosahedral Ti–Zr–Ni alloys under high pressure. They have shown that, under quasihydrostatic pressure, the hydrogenated Ti–Zr–Ni alloys remain icosahedral up to highest pressure, as found

previously for non-hydrogenated Ti–Zr–Ni quasicrystals [4–6]. The 6D parameter decreases monotonically for all the alloys, but more so for the hydrogenated alloys. The zero-pressure bulk modulus and its pressure derivative were determined by fitting, over the whole pressure range, a Murnaghan-type equation of state to the relative volume change V/V_0 and the zero-pressure bulk modulus obtained is $B_0 = 130 \pm 10$, 105 ± 10 , and 110 ± 20 GPa for H/M equal to 0, 0.32, and 1.45 respectively using a constant value of the first derivative B'_0 , equal to 5.5 ± 1 . Therefore, the icosahedral Ti–Zr–Ni phase may be more compressible after hydrogenation, but there is no clear difference for different H/M content. Moreover, the change obtained in the bulk modulus value is rather small, compared to the difference in the 6D parameter. These results are tentatively related to the increase of disorder observed in the local structure with hydrogenation in the same materials. They are also related to the unusual evolution of the specific volume per hydrogen atom obtained in Zr–Cu–Ni–Al QCs.

Acknowledgments

This work at Washington University was supported by the National Science Foundation (NSF) under grants DMR 97-05202 and DMR 00-72787.

References

- [1] Viano A M, Stroud R M, Gibbons P, McDowell A F, Conradi M S and Kelton K F 1995 *Phys. Rev. B* **51** 12 026
- [2] Köster U, Zander, Meinhardt J, Eliaz N and Eliezer D 1998 *Proc. 6th Int. Conf. on Quasicrystals (Tokyo, 1997)* ed T Takeuchi and T Fujiwara (Singapore: World Scientific) p 313
- [3] Kelton K F 1999 *Mater. Res. Soc. Symp. Proc.* **553** 471
- [4] Ponkratz U, Nicula R, Jianu A and Burkel E 1999 *J. Non-Cryst. Solids* **250–252** 844
- [5] Nicula R, Jianu A, Ponkratz U and Burkel E 2000 *Phys. Rev. B* **62** 8844
- [6] Sadoc A, Itié J P, Polian A, Kim J Y and Kelton K F 2000 *Proc. 7th Int. Conf. on Quasicrystals (Stuttgart, 1997); Mater. Sci. Eng. A* **294** 804
- [7] Sadoc A, Itié J P, Polian A and Kelton K F 2001 *Materials Research Society Fall Mtg (Boston, 2000); Mater. Res. Soc. Symp. Proc.* submitted
- [8] Kim W J, Gibbons P C, Kelton K F and Yelon W B 1998 *Phys. Rev. B* **58** 2578
- [9] Kim J Y, Gibbons P C and Kelton K F 1998 *J. Alloys Compounds* **266** 311
- [10] Le Toullec R, Pinceaux J P and Loubeyre P 1988 *High Pressure Res.* **1** 77
- [11] Piermarini G J, Block S, Barnett J D and Forman R A 1975 *J. Appl. Phys.* **46** 2774
- [12] Cahn J W, Shechtman D and Gratias D 1986 *J. Mater. Res.* **1** 13
- [13] Polian A, unpublished
- [14] Murnaghan F D 1944 *Proc. Natl Acad. Sci. USA* **30** 244
- [15] Sadoc A, Itié J P, Polian A, Berger C and Poon J S 1998 *Phil. Mag. A* **77** 115 and references therein
- [16] Sadoc A, Itié J P and Polian 2000 *Phil. Mag. A* **80** 2057
In figures 3 and 7, the triangles refer to the powder sample in silicone oil.
- [17] Amazit Y, Perrin B, Fischer M, Itié J P and Polian A 1997 *Phil. Mag. A* **75** 1677
- [18] Akahama Y, Mori Y, Kobayashi M, Kawamura H, Kimura K and Takeuchi S 1989 *J. Phys. Soc. Japan* **58** 2231
- [19] Akahama Y, Mori Y, Kobayashi M, Kawamura H, Kimura K and Takeuchi S 1991 *J. Phys. Soc. Japan* **60** 1988
- [19] Itié J P, Lefebvre S, Sadoc A, Capitan M J, Bessière, M, Calvayrac Y and Polian A 1996 *Proc. 5th Int. Conf. on Quasicrystals (Avignon, 22–26 May 1995)* ed C Janot and R Mosseri (Singapore: World Scientific) p 168
- [20] Sadoc, A, Itié J P, Polian A and Lefebvre S 1996 *Phil. Mag. B* **74** 629
- [21] Foster K, Leisure R G, Shaklee J B, Kim J Y and Kelton K F 1999 *Phys. Rev. B* **59** 11 132
- [22] Zander D, Köster U, Eliaz N and Eliezer D 2000 *Proc. 7th Int. Conf. on Quasicrystals (Stuttgart, 1997); Mater. Sci. Eng. A* **294** 112
- [23] Sadoc A, Kim J Y and Kelton K F 1999 *Phil. Mag. A* **79** 2763
- [24] Sadoc A, Kim J Y and Kelton K F 2000 *Phil. Mag. A* submitted
- [25] Faust K R, Pfitsch D W, Stojanovich N A, McDowell A F, Adolphi N L, Majzoub E H, Kim J Y, Gibbons P C and Kelton K F 2000 *Phys. Rev. B* **62** 11 444